

## Diffraction jets at H1

---

**Richard Polifka**\* †‡

*Charles University in Prague*

*E-mail:* polirlam@mail.desy.de

In this measurement, the cross section for inclusive jet production in diffractive deep-inelastic scattering is presented. The leading final state proton is detected in the H1 Forward Proton Spectrometer. The data have been collected during the HERA-II period. The data cover the range  $x_{IP} < 0.1$  in fractional proton longitudinal momentum loss,  $0. \leq |t| \leq 1.0 \text{ GeV}^2$  in squared four-momentum transfer at the proton vertex and  $4 \leq Q^2 \leq 110 \text{ GeV}^2$  in photon virtuality. The dijet topology is defined by two inclusive jets in the central region, found by the  $k_T$  cluster algorithm in the hadronic centre-of-mass frame. The data are compared to parton shower Monte carlo and to NLO predictions.

*XVIII International Workshop on Deep-Inelastic Scattering and Related Subjects*

*April 19 -23, 2010*

*Convitto della Calza, Firenze, Italy*

---

\*Speaker.

†On behalf of the H1 Collaboration.

‡The work was supported by the grant SVV-2010-261 309.

## 1. Introduction

Diffraction in high energy hadronic scattering is a process, in which the colliding particles remain intact after the interaction despite the fact, that a system is produced separated by a gap from the beam particles. For small momentum transfer the quantum numbers of the exchanged particle are those of the vacuum. This exchange particle is called pomeron. Diffraction is not only part of quantum chromodynamics, it is a unique tool for investigating parton dynamics as well.

In  $ep$  collisions at the HERA collider, the diffractive interaction is described as an interaction of the Pomeron  $IP$  emerging from the proton with a photon coming from the lepton vertex. In these events, two clearly separated systems are defined. The  $M_X$  system is the result of the  $\gamma^*IP$  interaction and is situated mainly in the central part of the detector. The  $M_Y$  system is associated with the outgoing proton or low mass dissociative system located around the beampipe in the direction of the outgoing proton. There are two experimental techniques to select diffractive events: the large rapidity gap method ( $LRG$ ) and tagging of the outgoing scattered proton. The  $LRG$  method imposes a cut on activity in the forward region, since the  $M_X$  system is situated mainly in the central and backward regions. Using only central detector information allows to gather high statistics, but the selected sample suffers of admixture of proton dissociative events. Selecting the outgoing proton in a forward detector allows a precise reconstruction of the diffractive variables, but the statistics are limited by low acceptance of such a detector. The fact that no cut on central detector activity is needed allows investigation of the diffractive hadronic final state in the forward region.

This analysis measures the diffractive dijet cross sections with tagged outgoing protons. It is the first measurement of dijets using tagged proton data in the history of the H1 experiment. The dijet cross sections with the longitudinal fraction of proton energy loss up to  $x_{IP} < 0.1$  are measured and compared to the predictions of diffractive parton distribution functions obtained with  $LRG$  measurement. The selection based on the tagged proton allows the investigation of the hadronic final state going into the forward direction. This fact allows measurement of jets separated by large pseudorapidity region which allows testing of DGLAP parton dynamics. In this measurement large values of  $z_{IP}$  are accessible, where direct pomeron processes are expected to contribute.

## 2. The H1 Detector

The H1 detector is one of the two  $4\pi$  detectors that belongs to the DESY facility. A detailed description can be found in [1], [2]. Only the Forward Proton Spectrometer used for measurement of the leading protons will be described in more detail in the following section.

### 2.1 The Forward Proton Spectrometer

For the purpose of diffractive physics, the detection of the outgoing protons is of extreme importance. For this purpose, the Forward Proton Spectrometer (FPS, see [3]) was built. The FPS consists of two stations: the horizontal one is located at 63m and 80m and the vertical one at 81m and 90m. Each station consists of two so called *Roman Pots*, the device that moves the detector. When taking data, the active region of the detector approaches the beam to about 1 cm. Each part of the horizontal and vertical stations consists of two identical subdetectors. These two subdetectors belong to one Roman pot. Each subdetector consists of two planes inclined by  $\pm 45$  degrees with

respect to the vertical pot axis. Each coordinate plane consists of five layers of 48 scintillating fibers in the horizontal stations and 20 fibers in the vertical stations, respectively. The fibers belonging to a read out plane are attached to multi-channel photomultipliers. The horizontal station is able to detect protons with an energy from 800 GeV up to 920 GeV (for HERA-II) which corresponds to the maximum value of  $x_P = 0.1$ .

### 3. Data Selection

#### 3.1 Kinematics

In order to describe DIS cross sections, the usual kinematic variables  $Q^2$  and  $y$  have to be defined as  $Q^2 = -q^2 = -(k' - k)^2$  and  $y = \frac{pq}{pk}$ .  $Q^2$  defines the photon virtuality at the lepton vertex,  $k$  ( $k'$ ) denotes the incoming (outgoing) lepton four momentum. The variable  $y$  defines the inelasticity of the proces. Both these observables require a precise measurement of the scattered lepton. Diffractive kinematics is represented by variables  $t$  and  $x_{IP}$ ,  $t = -(p' - p)^2$  and  $x_{IP} = 1 - \frac{E'_p}{E_p}$ . The  $p$  ( $p'$ ) stands for incoming (outgoing) proton four momentum. The variable  $x_{IP}$  defines the longitudinal momentum fraction lost by the proton and  $t$  is the squared four-momentum transfer at the proton vertex. The angular distribution of the jets is measured by the observable *pseudorapidity*  $\eta = -\ln \tan(\frac{\theta}{2})$ . The fraction  $z_{IP}$  of the pomeron momentum carried by the parton entering the hard scattering is  $z_{IP} = \frac{(Q^2 + M_{12}^2)}{x_{IP}ys}$ , where the  $M_{12}$  stands for the invariant mass of the dijet system,  $s$  for the squared  $ep$  centre-of-mass energy and the other variables as defined above.

#### 3.2 Selection

The analysis is performed on the data from the HERA-II operating period. It was taken in the years from 2005 to 2007 with an integrated luminosity  $L = 156 pb^{-1}$ . This subtrigger used for the data selection consists of a low level SpaCal condition for the energy of the scattered electron and of a requirement for a good reconstructed track in the *FPS* detector. For the good measurement of deep inelastic variables the precise selection of the scattered lepton is essential. Therefore, quality cuts on the scattered lepton and proton are applied. While measuring with the *FPS* detector, the background produced by halo protons has to be subtracted. Some events may fake the diffractive signal with a proton coming not from the interaction point but from the halo of the proton beam. These halo protons in *FPS* can be in coincidence with a standard DIS event in the central detector. For distinguishing between the background events and diffractive events, the variable  $E + P_Z$  has been defined. It sums the energy and momentum  $z$ -coordinate of all particles including the *FPS* proton. This observable should peak at twice the proton beam energy, i.e. at  $E + P_Z = 1840 GeV$ . The values of  $E + P_Z$  for background events lie above the diffractive peak, so a cut at  $E + P_Z < 1880 GeV$  has been applied. The background below the cut has been subtracted statistically. The phase space cuts are  $4 < Q^2 < 110 GeV^2$ ,  $0.05 < y < 0.7$  and  $x_{IP} < 0.1$ .

The jets are found with the *FastJet* [4]  $k_T$  cluster algorithm in the hadronic centre-of-mass system, where the cuts on transverse momenta are applied. Then they are boosted back to lab system and  $\eta$  cuts are applied to ensure the proper reconstruction of the jet constituents in the LAr calorimeter. The jet selection follows the conditions  $p_{T1}^* > 5 GeV$ ,  $p_{T2}^* > 4 GeV$  and  $-1 < \eta_{1,2} < 2.5$ , where the \* denotes an observable calculated in the hadronic centre-of-mass system.

### 3.3 Model Predictions

The cross sections are corrected to the level of stable hadrons in order to compare the results with theoretical predictions. For comparison, the Rapgap Monte Carlo and next-to-leading order calculations are used. The Rapgap3.1 Monte Carlo [5] uses leading order matrix elements, mimics the NLO behaviour with a running coupling constant  $\alpha_S$  and with parton showers. The NLO calculations have been done at the parton level with the NLOJET++ [6] program and corrected to the level of stable hadrons with hadronisation corrections obtained with RapGap. For the NLO predictions the variation of the factorisation and renormalisation scale  $\mu^2$  to  $2\mu^2$  and  $\mu^2/2$  leads to the estimation of scale uncertainties. The Rapgap Monte Carlo has been used to estimate the hadronization corrections uncertainties. For both theoretical comparisons, the diffractive parton density function H1 2006 Fit B [7], which assumes the resolved pomeron model [8],[9], has been used. This DPDF was extracted from the data selected by the LRG method. The correction for proton dissociation in the LRG sample is performed by scaling the predictions down by a factor 1.23 [10].

## 4. Results

Fig 1 shows the cross section measured differentially in  $\log x_{IP}$ . The measurement is compared to published data [11]. The published data are measured with the LRG method, hence the cross section has to be scaled down by the factor of 1.23 (see above). The cross section shows the extension of the phase space by using the FPS detector by a factor of 3 and proves the consistency of the two independent reconstruction methods for selecting diffractive events. The NLO calculation is consistent with the data. The Rapgap Monte Carlo with parton showers describes the shape of the data, but is off in normalisation.

The cross sections related to the jet observables, i.e.  $p_{T,1}^*$ ,  $p_{T,2}^*$ ,  $z_{IP}$  and  $\Delta\eta^*$  (see Fig. 2) are in general well described by the NLO predictions. The LO Monte Carlo with Parton Showers describes the shape of the data fairly well, but is off in normalisation. The deviation in the  $\Delta\eta^*$  distribution, i.e. the size of the gap between the two jets, in the last bin may be a hint for parton dynamics beyond DGLAP evolution equations. The resolved pomeron model represented by the NLO calculations is consistent with the data even in the highest  $z_{IP}$  bin, no hints for direct pomeron exclusive dijet production are observed.

The cross sections in the observable  $y$  (see Fig. 2) is in acceptable agreement with the NLO predictions within errors. The shape of the data is reproduced better by Rapgap Monte Carlo prediction than the NLO calculations, but is off in total normalisation.

## References

- [1] Abt, I. et al. *Nucl. Instrum. Meth.* **A386**, 310 (1997).
- [2] Abt, I. et al. *Nucl. Instrum. Meth.* **A386**, 348 (1997).
- [3] van Esch, P. et al. *Nucl. Instrum. Meth.* **A446**, 409 (2000).
- [4] Cacciari, M. and Salam, G. P. *Phys. Lett.* **B641** (2006) [hep-ph/0512210]
- [5] Jung, H. *Comp. Phys. Comm.* **86** 147 (1995).

- [6] Nagy, Z. and Trocsanyi, Z. *Phys. Rev. Lett.* **87** (2001) 082001.  
 [7] Aktas, A. et al. *Eur. Phys. J.* **C48**, 715-748 (2006).  
 [8] Ingelman, G. and Schlein, P. E. *Phys. Lett.* **B152**, 256 (1985).  
 [9] Donnachie, A. and Landshoff, P. V. *Phys. Lett.* **B191**, 309 (1987).  
 [10] Aktas, A. et al. *Eur. Phys. J.* **C48** (2006) 749-766, [arXiv:hep-ex/0606003v1]  
 [11] Aktas, A. et al. *Eur. Phys. J.* **C10** (2007) 42, [arXiv:0708.3217v1]

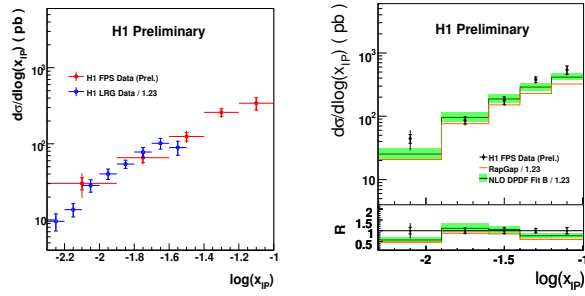


**Figure 1:** The cross section measured differentially in  $\log x_{IP}$ , the comparison to the published data [11] (left) to the NLO and Monte Carlo predictions. Data are presented with the statistical and systematical error combined in quadrature. The NLO predictions are presented with quadratically combined scale variations and hadronisation uncertainties. The total normalisation uncertainty is not shown. The  $R$  (lower part) stands for ratio of theory to the data. Data with corresponding errors are normalised to unity.

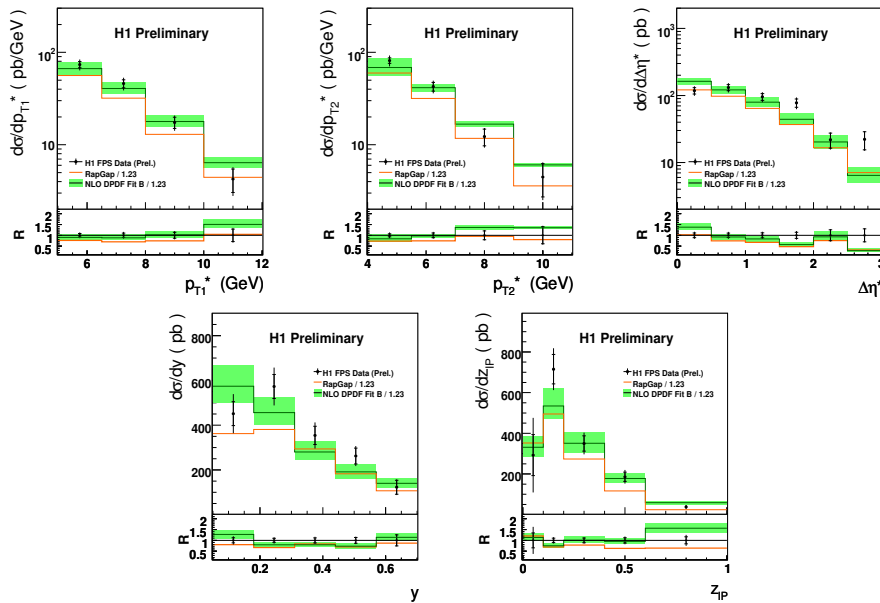


**Figure 2:** The  $p_{T,1}^*$  and  $p_{T,2}^*$ ,  $\Delta\eta^*$ ,  $y$  and  $z_{IP}$  differential cross sections. See caption of Fig. 1 for further details.